

# The Structure of Oxide Glasses: Insights from $^{17}\text{O}$ NMR

Philip J. Grandinetti and Ted M. Clark

Department of Chemistry, Ohio State University, 100 West, 18th Avenue, Columbus, OH 43210 USA

As a probe of local structure in network forming oxide glasses,  $^{17}\text{O}$  nuclear magnetic resonance (NMR) spectroscopy has been an invaluable tool [1–10]. The analysis of oxygen in these glasses is vital because their structure predominately consists of well-defined corner-sharing  $\text{SiO}_4$  tetrahedra connected in a continuous infinite three-dimensional network lacking long-range order. The interconnection of two tetrahedra involves a Si–O–Si bond angle, and two dihedral angles, and the variation in these angles is considered to be one of the main sources of disorder in a conventional melt quenched silicate glass.

The best approach for measuring Si–O–Si bond angle distributions is to use methods that provide a detailed and direct measurement of the local environment around oxygen. Unfortunately, the information obtainable from X-ray absorption spectroscopies has been limited for light backscattering atoms like oxygen [11]. In contrast, solid-state  $^{17}\text{O}$  NMR, specifically, the  $^{17}\text{O}$  quadrupolar coupling and chemical shift parameters provide a simple and direct probe of electronic structure, and is well suited for measuring the local structure around bridging oxygen [12–21].

With the development of 2D NMR methods that separate and correlate anisotropic and isotropic lineshapes [22–24], it is becoming increasingly possible to obtain local structural information for glasses via  $^{17}\text{O}$  NMR. In 1992, Farnan *et al.* [4] first demonstrated how the distribution of  $^{17}\text{O}$  NMR parameters can be measured in a silicate glass using 2D dynamic-angle spinning (DAS) NMR without any assumptions about the shape of the NMR parameter distributions. Additionally, they demonstrated that the  $^{17}\text{O}$  quadrupolar coupling parameter distribution can, in principle, be mapped into the Si–O–Si bond angle distribution in the glass.

A crucial aspect in these structural determinations is an understanding of the relationship between the measurable NMR parameters and the variations in local structure that influence the NMR parameters. The development of such relationships has been an ongoing task for oxygen in oxide glasses, with significant gains being made by the combination of computational methods and experimental investigation of a variety of oxygen environments in crystalline silicates.

For bridging oxygen, a number of structural features play a role in determining the  $^{17}\text{O}$  quadrupolar coupling

parameters, with the most significant features occurring in the first coordination sphere of the bridging oxygen. In the mid-1980's Oldfield and coworkers [25–27] clearly established on the basis of their  $^{17}\text{O}$  magic-angle spinning (MAS) NMR measurements that the electronegativity of the cations coordinated to a bridging oxygen atom is a primary factor influencing the magnitude of the  $C_q$ -parameter for the bridging oxygen. In a series of *ab initio* calculations on model clusters focusing on the silicate bridging oxygen linkage Tossell and coworkers [12–14] predicted simple trends for the  $^{17}\text{O}$  quadrupolar coupling parameters with Si–O–Si angle. These trends were later experimentally confirmed by Grandinetti *et al.* [17] in  $^{17}\text{O}$  DAS measurements on coesite.

Vermillion *et al.* [19] and Clark *et al.* [20] further refined this understanding by examining the effect of additional coordination of the bridging oxygen by network modifier alkali cations. Their findings, obtained using *ab initio* methods on model clusters representing typical bridging oxygen environments in lithium, sodium, and potassium silicates, suggested that the previously established trend in  $^{17}\text{O}$   $C_q$  with Si–O–Si angle is systematically shifted to lower magnitudes with increasing number and field strength of coordinating alkali cations. They also found that the previously established trend [12–15] in  $^{17}\text{O}$  quadrupolar coupling asymmetry parameter,  $\eta_q$ , with Si–O–Si angle is systematically shifted to higher values by the presence of one coordinating alkali cation, and only slightly shifted to higher values by the presence of two coordinating alkali cations.

In two related papers, Clark and Grandinetti [18, 28] used *ab initio* methods to study a number of clusters with the coordinating cations varied from Group III to Group VI and from Periods 2 to 4, while simultaneously varying the network forming cation–oxygen distance. A general trend, shown in Figure 1A, was observed that the magnitude of  $C_q$  increases linearly with increasing network forming cation–oxygen bond distance, and also increases with cation group number, as shown Figure 1B. These findings suggest that group number and cation–bridging oxygen distance can serve as a better predictor of the bridging oxygen quadrupole coupling constant than electronegativity differences [26, 27].

The observation that the magnitude of  $C_q$  increases linearly with increasing network forming cation–oxygen

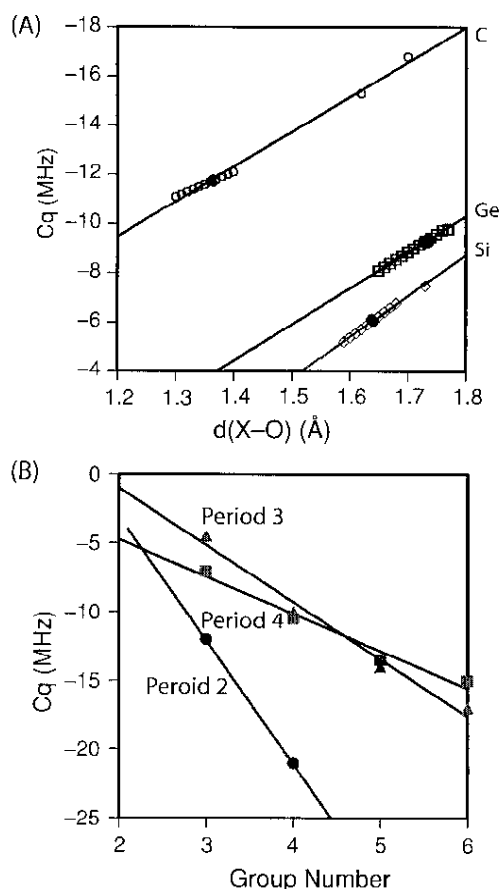


**Fig. 1.** (A) Comparison of bridging oxygen  $^{17}\text{O}$   $C_q$  values for the clusters  $(\text{OH})_3\text{T-O-T}(\text{OH})_3$ , where T = carbon, silicon, and germanium, as a function of  $d(\text{T-O})$ . (B) Bridging oxygen  $C_q$  dependence on the group number of coordinating cations for each period.  $C_q$  values are calculated for identical cation-oxygen distances and a bridging oxygen angle of  $180^\circ$ .

bond distance was investigated in more detail by Clark and Grandinetti for bridging oxygen atoms in silicates [21]. In this work, *ab initio* calculations were performed for model clusters to examine the dependence of  $^{17}\text{O}$  quadrupolar coupling parameters on both Si-O distance and Si-O-Si angle. This work demonstrated that the  $^{17}\text{O}$  quadrupolar coupling constant is dependent on both of these structural features, while  $\eta_q$  is primarily dependent on the Si-O-Si angle. Also, it is noteworthy that the strong linear dependence of  $C_q$  on Si-O distance helped explain the rather different angular trends for  $C_q$  found in coesite [17] and ferrierite [29], since the Si-O-Si angle and Si-O

distance correlations for these two materials are quite different [21].

Relationships between  $^{17}\text{O}$  quadrupolar coupling parameters and structure in silicates have also been examined using periodic density functional theory (DFT) calculations. These calculations, which are capable of describing quite accurately a system's electronic structure, have been performed for crystalline sodium silicates, the siliceous zeolite ferrierite, and also for plausible sodium silicate glasses that were generated using molecular dynamics [30,31]. These calculations generally support the previously established trends, i.e.  $C_q$  decreases in magnitude with decreasing Si-O-Si angle and Si-O distance, whereas  $\eta_q$  depends only on Si-O-Si angle. Additionally, these investigations found no dependence of the bridging oxygen  $C_q$  upon the number of coordinating alkali cations, a finding in contrast to that reported using modeling clusters [19,20].

Overall, it has become clear that first coordination sphere structural features that appear to be most important in determining the  $^{17}\text{O}$  quadrupolar coupling parameters of the bridging oxygen are the nature of the two coordinating network forming cations, the T-O-T' linkage angle, the T-O bond distances, and the nature and number of coordinating network modifier cations. Contributions from beyond the first coordination sphere of the bridging oxygen appear to be secondary in importance. For example, Xue and Kanzaki [16] performed *ab initio* calculations employing clusters expanded out to four coordination spheres to model each of the silicate bridging oxygen linkages in coesite and obtained a slightly improved agreement with the experimental trends, with corrections on the order of a few percent in the  $^{17}\text{O}$   $C_q$  and  $\eta_q$  values.

Equations proposed to summarize the important structural features for the determination of the  $^{17}\text{O}$  quadrupolar coupling parameters are

$$C_q(\Omega, n_M) = a \left( \frac{1}{2} + \frac{\cos \Omega}{\cos \Omega - 1} \right)^\alpha + n_M \Delta C_q^M + m_d(d_{\text{T-O}} - d_{\text{T-O}}^0) \quad (1)$$

$$\eta_q(\Omega) = b \left( \frac{1}{2} - \frac{\cos \Omega}{\cos \Omega - 1} \right)^\beta + \Delta \eta_q^M(n_M), \quad (2)$$

where  $\Omega$  is the Si-O-Si bond angle,  $d_{\text{T-O}}$  is the average silicon-oxygen bond distance, and the terms  $n_M \Delta C_q^M$  and  $\Delta \eta_q^M(n_M)$  account for contributions from modifier cations coordinated to the bridging oxygen. These expressions are not unique in their ability to describe these relationships, and other expressions have been used previously [4,14,15].

Clark and Grandinetti [21] performed a least-squares fit of Equations (1) and (2) to the experimental values for coesite [17], cristobalite [32], and  $\alpha$ -quartz [33] as

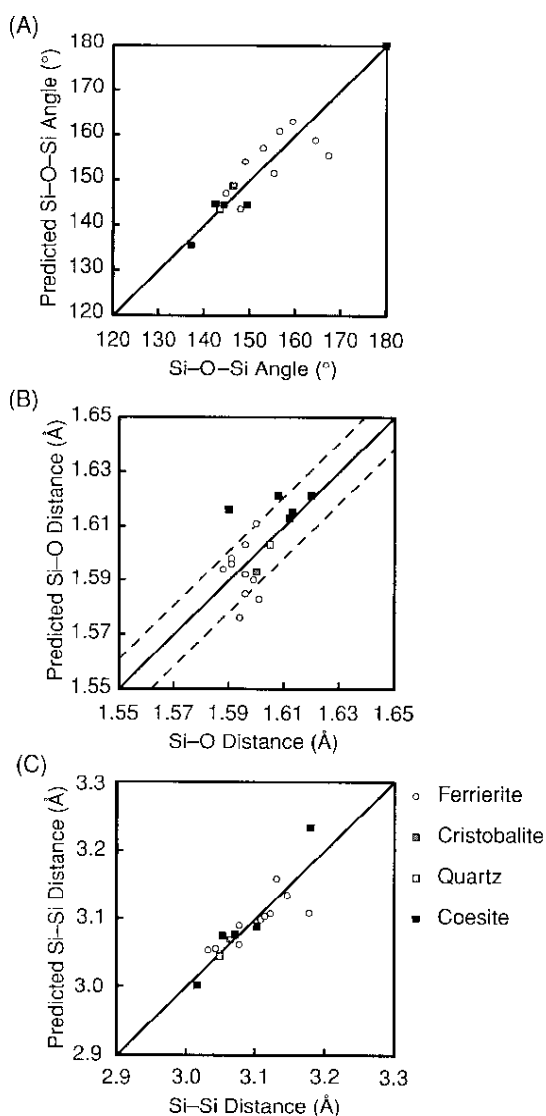


**Fig. 2.** Comparison between  $^{17}\text{O}$  quadrupolar coupling predicted (A) Si–O–Si angle, (B) Si–O distance, and (C) Si–Si distance with corresponding quantities reported from X-ray crystallography [40–42]. Solid diagonal lines represent perfect agreement. Best fit parameters for Equations (1) and (2) are  $\alpha' = -6.53$  MHz,  $\alpha' = 1.80$ ,  $m_d = -12.86$  MHz/Å,  $d_{17\text{O}}^0 = 1.654$  Å,  $b = 4.73$ ,  $\beta = 1.12$ .

well as the *ab initio* predicted values for ferrierite [29] and obtained the parameter values given in the caption of Figure 2. The resulting parameterized equations describe the relationships between the  $^{17}\text{O}$  quadrupolar coupling

parameters and the relevant structural features in the first coordination sphere for a bridging oxygen atom in the absence of modifier cations. The precision of these relationships can be seen in Figure 2, where the Si–O–Si angles and Si–O distances predicted by these expressions are shown versus the actual values. Close agreement between predicted and reported values are demonstrated, even though only two structural variables are considered, i.e. the average bond distance and the bond angle. Here, the Si–O–Si angles in Figure 2A are predicted from  $\eta_q$  alone and, with the Si–O–Si angle determined, Equation (1) is used to predict the Si–O distance from  $C_q$ , as shown in Figure 2B. After having determined the Si–O distance for a given angle, it is also possible to determine the Si–Si distance.

It is noteworthy that not only the quadrupolar coupling constant and asymmetry parameter can be used to measure the Si–O–Si angle and Si–O distance, but also the simultaneous measurement of  $C_q$  and  $\eta_q$  for each bridging oxygen site can be used to obtain the correlation between Si–O–Si angle and Si–O distance. This has significant impact for determining two-dimensional structural distributions around bridging oxygen in silicate glasses. This approach requires a good measurement of the quadrupolar asymmetry parameter, which has been historically been more difficult to measure than the quadrupolar coupling constant. Fortunately, this situation has been improved with the development of techniques such as Rotor Assisted Population Transfer (RAPT) [34–37] for enhancing the sensitivity of the MAS detected DAS [17,38,39] experiment, which allows overlapping anisotropic  $^{17}\text{O}$  central transition lineshapes to be separated.

Figure 3A is the recently reported  $^{17}\text{O}$  RAPT/MAS-detected DAS spectrum of silica glass [43]. From a least-square analysis of the  $^{17}\text{O}$  2D DAS spectrum a three-dimensional histogram, correlating the  $\delta_{cr}$  (chemical shift),  $C_q$ , and  $\eta_q$  of  $^{17}\text{O}$ , was obtained. A projection of this three dimensional histogram, showing the two-dimensional correlation between  $C_q$  and  $\eta_q$  for silica glass, along with corresponding one-dimensional projections is shown in Figure 3B. With the aid of Equations (1) and (2), the experimental  $C_q$  and  $\eta_q$  histograms were mapped into the two-dimensional histogram of the Si–O–Si angle versus the Si–O distance, shown in Figure 3C. This result is the first experimentally measured two-dimensional structural distributions in a glass, and illustrates nearly strong linear correlations between the Si–O–Si angle and Si–O distance in silica glass.

Significant insights into the structure of silicate glasses are now made possible by an analysis using this methodology. For example, in the case of silica glass, it is remarkable that a strong positive correlation is observed between Si–O distance and Si–O–Si bond angle. This trend was unexpected since it is *opposite* of that generally found in crystalline  $\text{SiO}_2$  polymorphs, as shown in

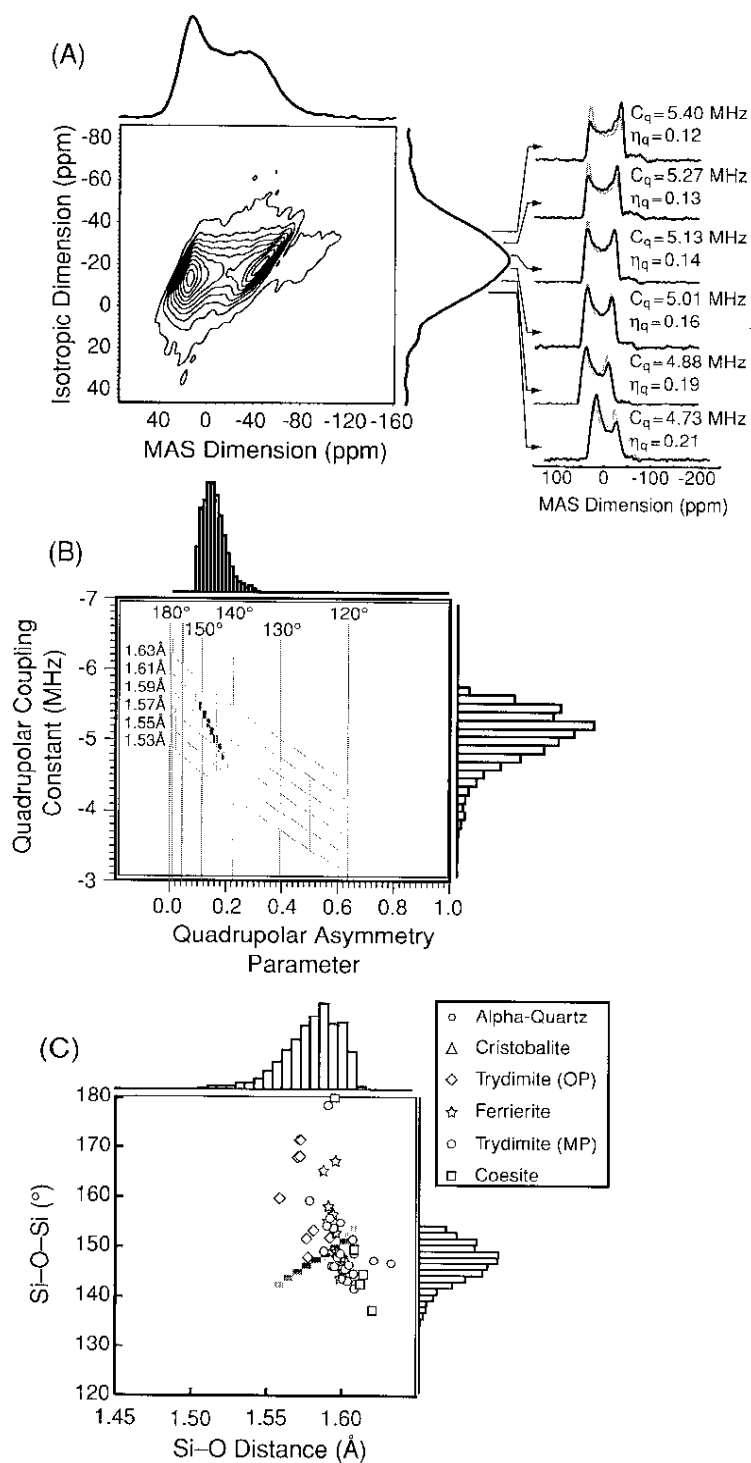


**Fig. 3.** (A) Experimental 2D  $^{17}\text{O}$  RAPT/MAS-detected DAS spectrum of  $\text{SiO}_2$  at 9.4 T along with experimental 1D projections onto the MAS and isotropic dimensions. Shown on the right are selected experimental cross sections along with best fit simulations. (B) Two-dimensional histograms along with the corresponding one-dimensional projection showing the correlation between  $C_q$  and  $\eta_q$ . Grid lines shown were obtained from Equations (1) and (2) by varying Si-O distance with Si-O-Si angle held constant and the Si-O-Si angle with the Si-O distance held constant. (C) 2D histograms of Si-O-Si angle versus Si-O distance for silica glass derived from NMR parameter distributions, and for various crystalline polymorphs.

Figure 3C. Also, the resulting Si–O–Si bond angle distribution, which peaks at  $147^\circ$  with a standard deviation of  $3.8^\circ$ , is noteworthy for its narrowness in comparison with distributions determined by diffraction or Si-29 NMR measurements [44–46].

In conclusion,  $^{17}\text{O}$  NMR is proving to be an extremely robust probe of structure in silicate glasses. As the relationship between the  $^{17}\text{O}$  NMR parameters and structure has become increasingly well-understood, it is now possible to apply this knowledge for the interpretation of the two-dimensional NMR spectra of disordered materials. This has led to the experimental determination of correlated structural distributions for oxygen sites in glasses, a significant achievement that is not presently possible by other experimental techniques. With the continued application of this methodology, it will be possible to gain a more complete understanding of many glasses of scientific and technological importance.

## References

- Jellison GE, Panek LW, Bray PJ, Rouse GB. Determinations of structure and bonding in vitreous  $\text{B}_2\text{O}_3$  by means of  $^{10}\text{B}$ ,  $^{11}\text{B}$ , and  $^{17}\text{O}$  NMR. *J. Chem. Phys.* 1977;66:802.
- Geissberger AE, Bray PJ. Determinations of structure and bonding in amorphous  $\text{SiO}_2$  using  $^{17}\text{O}$  NMR. *J. Non-Cryst. Solids.* 1983;54:121.
- Youngman RE, Haubrich ST, Zwanziger JW, Janicke MT, Chmelka BF. Short- and intermediate-range structural ordering in glassy boron oxide. *Science.* 1995;269:1416.
- Farnan I, Grandinetti PJ, Baltisberger JH, Stebbins JF, Werner U, Eastman MA, Pines A. Quantification of the disorder in network-modified silicate glasses. *Nature.* 1992;358:31–5.
- Wang S, Stebbins JF. On the structure of borosilicate glasses: A triple-quantum magic-angle spinning  $^{17}\text{O}$  nuclear magnetic resonance study. *J. Non Cryst. Solids.* 1998;231:286–90.
- Zhao P, Kroeker S, Stebbins JF. Non-bridging oxygen sites in barium borosilicate glasses: results from  $^{11}\text{B}$  and  $^{17}\text{O}$  NMR. *J. Non-Cryst. Solids.* 2000;276:122–31.
- Florian P, Vermillion KE, Grandinetti PJ, Farnan I, Stebbins JF. Cation distribution in mixed alkali disilicate glasses. *J. Am. Chem. Soc.* 1996;118:3493–7.
- Stebbins JF, Oglesby JV, Xu Z. Disorder among network-modifier cations in silicate glasses: New constraints from triple-quantum  $^{17}\text{O}$  NMR. *Am. Mineral.* 1997;82:1116–24.
- Stebbins JF, Lee SK, Oglesby JV. Al–O–Al oxygen sites in crystalline aluminates and aluminosilicate glasses: High-resolution oxygen-17 NMR results. *Am. Mineral.* 1999;84:983–6.
- Lee SK, Musgrave CB, Zhao P, Stebbins JF. Topological disorder and reactivity of borosilicate glasses: Quantum chemical calculations and  $^{17}\text{O}$  and  $^{11}\text{B}$  NMR study. *J. Phys. Chem. B.* 2001;105:12583–95.
- Elliott SR. Non-diffraction spectroscopic probes of the structure of amorphous solids. *J. Non-Cryst. Solids.* 1990;123:149.
- Tossell JA, Lazzeretti P. *Ab Initio* calculations of oxygen nuclear quadrupolar coupling constants and oxygen and silicon NMR shielding constants in molecules containing Si–O bonds. *Chem. Phys. Lett.* 1987;112:205.
- Tossell JA, Lazzeretti P. Calculation of NMR parameters for bridging oxygens in  $\text{H}_3\text{T–O–T}'\text{H}_3$  linkages (T, T' = Al, Si, P), for oxygen in  $\text{SiH}_3\text{O}^-$ ,  $\text{SiH}_3\text{OH}$  and  $\text{SiH}_3\text{OMg}^+$  and for bridging fluorine in  $\text{H}_3\text{SiFSiH}_3^+$ . *Phys. Chem. Minerals.* 1988;15:564.
- Lindsay CG, Tossell JA. *Ab Initio* calculations of  $^{17}\text{O}$  and  $^n\text{T}$  NMR parameters ( $^n\text{T} = ^{31}\text{P}, ^{29}\text{Si}$ ) in  $\text{H}_3\text{TOTH}_3$  dimers and  $\text{T}_3\text{O}_9$  trimeric rings. *Phys. Chem. Minerals.* 1991;18:191.
- Sternberg U. The bond-angle dependence of the asymmetry parameter of the oxygen-17 electric field gradient tensor. *Solid State NMR.* 1993;2:181.
- Xue X, Kanzaki M. An ab initio calculation of  $^{17}\text{O}$  and  $^{29}\text{Si}$  NMR parameters for  $\text{SiO}_2$  polymorphs. *Solid State NMR.* 2000;16:245–259.
- Grandinetti PJ, Baltisberger JH, Werner U, Pines A, Farnan I, Stebbins JF. Solid-state  $^{17}\text{O}$  magic-angle and dynamic-angle spinning NMR study of coesite. *J. Phys. Chem.* 1995;99:12341–8.
- Clark TM, Grandinetti PJ. Factors influencing the  $^{17}\text{O}$  quadrupole coupling constant in bridging oxygen environments. *Solid State NMR.* 2000;16:55–62.
- Vermillion KE, Florian P, Grandinetti PJ. Relationships between bridging oxygen  $^{17}\text{O}$  quadrupolar coupling parameters and structure in alkali silicates. *J. Chem. Phys.* 1998;108(17):7274–7285.
- Clark TM, Grandinetti PJ, Florian P, Stebbins JF. An  $^{17}\text{O}$  NMR investigation of crystalline sodium metasilicate: Implications for the determinations of local structure in alkali silicates. *J. Phys. Chem. B.* 2001;105:12257–65.
- Clark TM, Grandinetti PJ. Dependence of bridging oxygen O–17 quadrupolar coupling parameters on Si–O distance and Si–O–Si angle. *J. Phys. Condensed Matter.* 2003;15:S2387–95.
- Bax A, Szeverenyi NM, Maciel GE. Correlation of isotropic shifts and chemical shift anisotropies by two-dimensional Fourier-transform magic-angle hopping NMR spectroscopy. *J. Magn. Reson.* 1983;52:147.
- Terao T, Fujii T, Onodera T, Saika A. Switching-angle sample -spinning NMR spectroscopy for obtaining powder-pattern-resolved 2D spectra: Measurements of  $^{13}\text{C}$  chemical-shift anisotropies in powdered 3,4-dimethoxybenzaldehyde. *Chem. Phys. Lett.* 1984;107:145.
- Mueller KT, Sun BQ, Chingas GC, Zwanziger JW, Terao T, Pines A. Dynamic-angle spinning of quadrupolar nuclei. *J. Magn. Reson.* 1990;86:470.
- Schramm S, Oldfield E. High-resolution oxygen-17 NMR of solids. *J. Am. Chem. Soc.* 1984;106:2502.
- Timken HKC, Janes N, Turner GL, Lambert SL, Welsh LB, Oldfield E. Solid-state oxygen-17 nuclear magnetic resonance spectroscopic studies of zeolites and related systems. *J. Am. Chem. Soc.* 1986;108:7236.
- Timken HKC, Schramm SE, Kirkpatrick RJ, Oldfield E. Solid-state oxygen-17 nuclear magnetic resonance spectroscopic studies of alkaline earth metasilicates. *J. Phys. Chem.* 1987;91:1054–8.

28. Clark TM, Grandinetti PJ. Relationships between bridging oxygen  $^{17}\text{O}$  quadrupolar coupling parameters and structure in germanates. *J. Non-Cryst. Solids*. 2000;265:75–82.
29. Bull LM, Bussemer B, Anupold T, Reinhold A, Samoson A, Sauer J, Cheetham AK, Dupree R. A high-resolution  $^{17}\text{O}$  and  $^{29}\text{Si}$  NMR study of zeolite siliceous ferrierite and ab initio calculations of NMR parameters. *J. Am. Chem. Soc.* 2000;122:4948–58.
30. Charpentier T, Ispas S, Profeta M, Mauri F, Pickard CJ. First-principles calculation of  $^{17}\text{O}$ ,  $^{29}\text{Si}$ ,  $^{23}\text{Na}$  NMR spectra of sodium silicate crystals and glasses. *J. Phys. Chem. B*. 2004;108:4147–61.
31. Profeta M, Mauri F, Pickard CJ. Accurate first principles prediction of  $^{17}\text{O}$  NMR parameters in  $\text{SiO}_2$ : Assignment of the zeolite ferrierite spectrum. *J. Am. Chem. Soc.* 2003;125:541–8.
32. Spearing DR, Farman I, Stebbins JF. Dynamics of the alpha-beta phase transitions in quartz and cristobalite as observed by in situ high temperature Si-29 NMR and O-17 NMR. *Phys. Chem. Miner.* 1992;19(5):307–21.
33. Dupree R. Nuclear magnetic resonance as a structural probe of  $\text{SiO}_2$ . In: R. Devine, JP. Durand, E. Dooryhee (Eds), *Structure and Imperfections in Amorphous and Crystalline  $\text{SiO}_2$* , John Wiley, pp. 107–20, 2000.
34. Kwak H-T, Prasad S, Clark TM, Grandinetti PJ. Selective suppression and excitation of solid-state NMR resonances based on quadrupole coupling constants. *J. Magn. Reson.* 2003;160:107–13.
35. Yao Z, Kwak H-T, Sakellariou D, Emsley L, Grandinetti PJ. Sensitivity enhancement of the central transition NMR signal of quadrupolar nuclei under magic-angle spinning. *Chem. Phys. Lett.* 2000;327:85–90.
36. Kwak H-T, Prasad S, Yao Z, Grandinetti PJ, Sachleben JR, Emsley L. Enhanced sensitivity in RIACT/MQ-MAS NMR experiments using rotor assisted population transfer. *J. Magn. Reson.* 2001;150:71–80.
37. Prasad S, Kwak HT, Clark T, Grandinetti PJ. A simple technique for determining nuclear quadrupole coupling constants using RAPT solid-state NMR spectroscopy. *J. Am. Chem. Soc.* 2002;124(18):4964–5.
38. Chmelka BF, Mueller KT, Pines A, Stebbins J, Wu Y, Zwanziger JW. Oxygen-17 NMR in solids by dynamic-angle spinning and double rotation. *Nature*. 1989;339:42–3.
39. Mueller KT, Wooten EW, Pines A. Pure-absorption-phase dynamic-angle spinning. *J. Magn. Reson.* 1990;92:620.
40. Geisinger KL, Spackman MA, Gibbs GV. Exploration of structure, electron density distribution, and bonding in coesite with fourier and pseudo atom refinement methods using single-crystal X-ray diffraction data. *J. Phys. Chem.* 1987;91:3237.
41. Downs RT, Palmer DC. The pressure behavior of alpha-cristobalite. *Am. Mineral.* 1994;79(1–2):9–14.
42. Kihara K. An X-ray study of the temperature dependence of the quartz structure. *Eur. J. Mineral.* 1990;2(1):63–77.
43. Clark TM, Grandinetti PJ, Florian P, Stebbins JF. Correlated structural distributions in silica glass. *Physical Rev. B*. 2004;70.
44. Mozzi RL, Warren BE. The structure of vitreous silica. *J. Appl. Cryst.* 1969;2:164–72.
45. Poulsen HF, Neuefeind J, Neuman H-B, Schneider JR, Zeidler MD. Amorphous silica studied by high energy X-ray diffraction. *J. Non Cryst. Solids*. 1995;188:63–74.
46. Mauri F, Pasquarello A, Pfrommer BG, Yoon Y-G, Louie SG. Si–O–Si bond-angle distribution in vitreous silica from first-principles  $^{29}\text{Si}$  NMR analysis. *Phys. Rev. B*. 2000;62(8):4786–9.